Fully Kinetic Fokker-Planck Model of Thermal Smoothing in Nonuniform Laser-Target Interactions

M. J. Keskinen

Charged Particle Physics Branch, Plasma Physics Division, Naval Research Laboratory, Washington, D.C. 20375, USA

(Received 5 November 2008; revised manuscript received 23 January 2009; published 30 July 2009)

Using a fully kinetic 2D Fokker-Planck model, the generation and evolution of ion density perturbations from nonuniform laser deposition in a plasma slab have been studied. It is found that significant smoothing of the ion density perturbations from nonuniform optically smoothed single beam laser deposition can be achieved on hydrodynamic times scales over a range of scale sizes. In addition, it is observed that the Fokker-Planck model predicts more smoothing than the hydrodynamic Spitzer model.

DOI: 10.1103/PhysRevLett.103.055001 PACS numbers: 52.65.Ff, 52.38.Dx, 52.50.Jm

Energy transport in laser-produced plasmas is an important issue in current high energy density plasma research, e.g., inertial confinement fusion (ICF) [1,2], femtosecond laser interactions with solids, and laboratory simulations of astrophysical phenomena using lasers.

In ICF, laser energy, absorbed in the hot, low-density corona, must be effectively conducted toward colder, higher-density regions of the target. A large inward heat flux from the critical surface, toward higher-density regions, implies that newly heated material at the surface of the cold target will expand outward rapidly leading to large fuel compression. Large compressions can lead to higher fusion gains. A limitation in ICF is pellet degradation and disruption due to the Rayleigh-Taylor (RT) instability where a hot, low-density plasma is used to compress and accelerate a cold, high-density plasma. The RT instability can be seeded by laser nonuniformities from single or multiple beams and target surface irregularities [1,2]. Single beam nonuniformities are the most detrimental to RT seeding and contribute to imprint through perturbations in the laser-driven shock front and acceleration in the postshock region. Short wavelength laser nonuniformities $\delta I/I$ may be reduced [1,2] due to thermal diffusion and smoothing such that $\delta P/P \leq \delta I/I$, where $\delta P/P$ is the pressure nonuniformity at the ablation surface which can seed the RT instability. However, longer wavelength laser nonuniformities may not be reduced by thermal diffusion alone [3,4]. In order to reduce the amplitudes of the laser uniformities, techniques for laser optical smoothing have been developed, e.g., induced spatial incoherence [5], spectral dispersion [6], and distributed phase plates [7].

Models for nonuniform laser-driven spatial and temporal heat flow evolution, over a large range of scale sizes, are important for ICF. It is well known that the measured heat flux is [8] below the flux predicted by classical electron thermal conduction. Strong inhibition of thermal transport below classical thermal conduction seems to exist in both long and short pulse laser deposition and in both high- and low-Z plasmas. In addition, the measured heat transport seems to be reduced both inward toward higher density regions and laterally toward the exterior. Several models have been advanced to explain the reduced heat flux in ICF experiments, e.g., ion acoustic turbulence [9], dc magnetic field effects [10], and kinetic theory in steep temperature gradients [11–15]. It has been shown [16,17] that hydrodynamic fluid models are not accurate to describe heat flow when $k\lambda_{\mathrm{mfp}} \geq 1/80$, where $2\pi k^{-1}$ is the scale size of the temperature or pressure and λ_{mfp} is the collisional mean free path. When this inequality is fulfilled, a kinetic model, e.g., a Vlasov Fokker-Planck (FP) formulation, must be used. Since the ion-ion collision time is typically larger than the laser coherence time and electron-ion energy transfer time, the ion distribution function may have non-Maxwellian features necessitating an ion kinetic model.

Some initial work has been performed using both hydrodynamic fluid models [3,18–20] and FP models [16,21], to study thermal smoothing and heat flow generated by nonuniform, inhomogeneous laser deposition for ICF applications. Previous FP studies [16,21] have been primarily devoted to the problem of the smoothing of electron temperature perturbations with a single scale size resulting from nonuniform laser deposition. The smoothing of ion density perturbations, resulting from nonuniform laser deposition, have not been studied quantitatively using FP models over a range of scale sizes. These ion density perturbations, at the ablation surface, can seed longer time scale Rayleigh-Taylor instabilities. However, laser deposition, resulting from optically smoothed lasers, can be structured over a broad range of spatial and temporal scales [5–7]. An outstanding problem is a kinetic model for the generation and evolution of ion density perturbations when $k\lambda_{\mathrm{mfp}} \geq 1/80$.

The objective of this Letter is to study ion density perturbations, using a fully kinetic FP model, resulting from simulated nonuniform optically smoothed laser deposition for a wide range of scale sizes. It is found that significant smoothing of ion density perturbations can be achieved on hydrodynamic time scales for a range of spatial scale sizes.

It is assumed that, to lowest order, the electron and ion distribution functions f are weakly anisotropic. As a result, we make the standard decomposition [22] with $f_\alpha = f_{0\alpha} + (v/v)\cdot \mathbf{f}_{1\alpha}$ with $\alpha = e, i$. For the electrons, in the frame of the ions:

$$\frac{df_{0e}}{dt} + \frac{v}{3}\nabla\cdot\mathbf{f}_{1e} - \nabla\cdot\mathbf{v}_i\frac{v}{3}\frac{\partial f_{0e}}{\partial v} + \frac{1}{3v^2}\frac{e}{m_e}\frac{\partial}{\partial v}[v^2(\mathbf{E}+\mathbf{E}_p)\cdot\mathbf{f}_{1e}] = \frac{Y_{ee}}{v^2}\frac{\partial}{\partial v}\left(A_{1e}f_{0e} + A_{2e}\frac{\partial f_{0e}}{\partial v}\right) + S, \quad (1)$$

$$\frac{\partial \mathbf{f}_{1e}}{\partial t} + v\nabla f_{0e} + \frac{e}{m_e}(\mathbf{E}+\mathbf{E}_p)\frac{\partial f_{0e}}{\partial v} = -\nu_{ei}^*\mathbf{f}_{1e}, \quad (2)$$

where $Y_{ee} = 4\pi(e^2/4\pi m_e)^2\ln\Lambda_{ee}$, the laser heating source term S can be written as $S = (Y_{ee}/v^2)\partial/\partial v[(n_i/6v)\times(Z^2\ln\Lambda_{ei}/\ln\Lambda_{ee})(1/\omega^2+\nu_{ei}^2)(e\mathbf{E}_0^2/m_e)^2]\partial f_{0e}/\partial v$, and $d/dt = \partial/\partial t + \mathbf{v}_i\cdot\nabla$. In addition, $\nu_{ei}^* = (4\pi\phi ne^4Z^*/m^2v^3)\ln\Lambda$, $\nu_{ee} = (4\pi ne^4/m^2v^3)\ln\Lambda$, $\phi = (Z^*+4.2)/(Z^*+0.24)$, and $Z^* = \langle Z^2\rangle/\langle Z\rangle$. Here the angle brackets denote an average over all ion species. A CH plasma is considered with $Z = 4$ and $Z^* = 5.3$. In Eq. (1), $\mathbf{v}_i$ is the average ion velocity derived from Eqs. (4) and (5). The quantities A_{1e} and A_{2e} have been previously defined [16,22]. The ponderomotive electric field $\mathbf{E}_p = (e/4m_e\omega^2)\nabla|\mathbf{E}_0|^2$. In Eqs. (1) and (2), $\mathbf{E}$ is taken to be electrostatic, and $\mathbf{E}_0$ is the laser electromagnetic electric field. Here S represents laser inverse bremsstrahlung absorption using the Langdon prescription [23].

The laser electromagnetic field is computed using a wave equation for the slow evolution of the wave field. The equation for the slow E_0 can be written

$$\left[\frac{\partial}{\partial t} - \frac{ic^2}{2\omega_0}\left(\frac{\partial^2}{\partial x^2}+\frac{\partial^2}{\partial z^2}\right) - i\omega_0(\epsilon_r - i\epsilon_i)\right]E_0 = 0, \quad (3)$$

where $\epsilon_r = 1 - n_e(z)/n_c$ and $\epsilon_i = (\nu_{ei}/\omega_0)n_e(z)/n_c$. In the transverse x direction, the wave numbers k_x for the spectral content of the laser electromagnetic field are constructed to simulate a set of beamlets generated by optical smoothing. The beamlets are then overlapped at the target plane using a lens of focal length f. The diffraction profile at the target plane will have a width $d = 2\lambda f/D_1$, where λ is the laser wavelength and D_1 is the beamlet width in which the laser intensity is assumed uniform. The transverse wave numbers are then given by $k_{xn} = nD_1/\lambda f$ with $n = 1, 2, \ldots$. In this preliminary study, $f = 40$ m, $\lambda = 0.25$ μm, and $D_1 = 75$ mm so that $d = 200$ μm. The set of transverse wavelengths used are $\lambda_n = 100$ μm$/n$ with $n = 1, \ldots, 40$. The complex amplitude of each beamlet is taken to obey Gaussian probability statistics with independent random fluctuations with a coherence time τ_c of 2 ps. A range of laser rise times of 10–100 ps was used after which the laser intensity was held constant.

For the two ion species we have

$$\frac{\partial f_{0i}}{\partial t} + \frac{v}{3}\nabla\cdot\mathbf{f}_{1i} - + \frac{1}{3v^2}\frac{Ze}{m_i}\frac{\partial}{\partial v}(v^2\mathbf{E}\cdot\mathbf{f}_{1i}) = \frac{Y_{ii}}{v^2}\frac{\partial}{\partial v}\left(A_{1i}f_{0i} + A_{2i}\frac{\partial f_{0i}}{\partial v}\right) + S_{ie}, \quad (4)$$

$$\frac{\partial \mathbf{f}_{1i}}{\partial t} + v\nabla f_{0i} + \frac{eZ\mathbf{E}}{m_i}\frac{\partial f_{0i}}{\partial v} = -\nu_{ie}\mathbf{f}_{1i}, \quad (5)$$

where $S_{ie} = -(m_e/m_i)(\nu_{ei}/v^2)\partial/\partial v[(v^2T_e/m_i)\partial f_{0i}/\partial v + v^3 f_{0i}]$.

The electric field $\mathbf{E}$ in Eqs. (1), (2), (4), and (5) is found from the zero current condition, i.e., $\mathbf{J} = 0$. We have numerically solved the model equation set consisting of Eqs. (1)–(5). The 2D fully kinetic Fokker-Planck code is solved using an alternating-direction implicit method. The peak vacuum laser intensity is 2×10^{14} W/cm^2 and is assumed to be normally incident in the z direction. The plasma parameters used are such that the ion acoustic transit time $t_s \simeq 50$–125 ps and the thermal diffusion time $t_{\rm th} \simeq 20$–100 ps.

Figure 1 shows the initial electron temperature and density profiles used in the simulation. The critical surface is located initially at approximately $z = 100$ μm. The ablation surface is located initially at approximately $z = 240$ μm. The initial electron temperature T_e is taken to be 230 eV with the initial ion temperature $T_i = 0$. The initial temperature and density are assumed to be uniform in the transverse x direction.

Figure 2 gives a snapshot of the longitudinal and transverse intensity profiles at $t = 100$ ps used to simulate the laser deposition. The longitudinal structure is consistent with an Airy pattern, while the transverse structure is random in both space and time and is due to simulated optical smoothing. These intensity profiles are used in the source term in Eq. (1). A single Gaussian beam with a full width at half maximum of 80 μm is used.

Figure 3 shows the 2D variation of the FP electron temperature T_e at $t = 420$ ps after the peak of the laser pulse using a laser coherence time of 2 ps. The evolution of the electron temperature also shows both longitudinal and transverse structure. It is found that ponderomotive effects are important only in the underdense plasma, i.e., for $z \le 100$ μm. Significant smoothing of the electron temperature perturbations is seen from the critical to ablation surface.

Figure 4 shows the 2D variation of the ion density n_i at $t = 420$ ps. It is found that structure near the critical

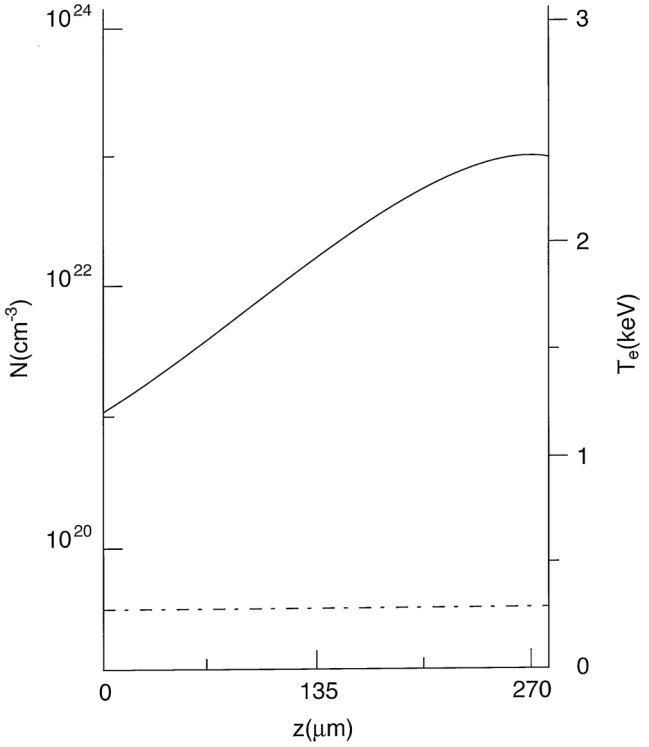

FIG. 1. Plot of initial electron temperature (dashed-dotted line) and density (solid line) vs z. Laser is incident from the left. The critical surface is approximately located at $z = 100$ μm.

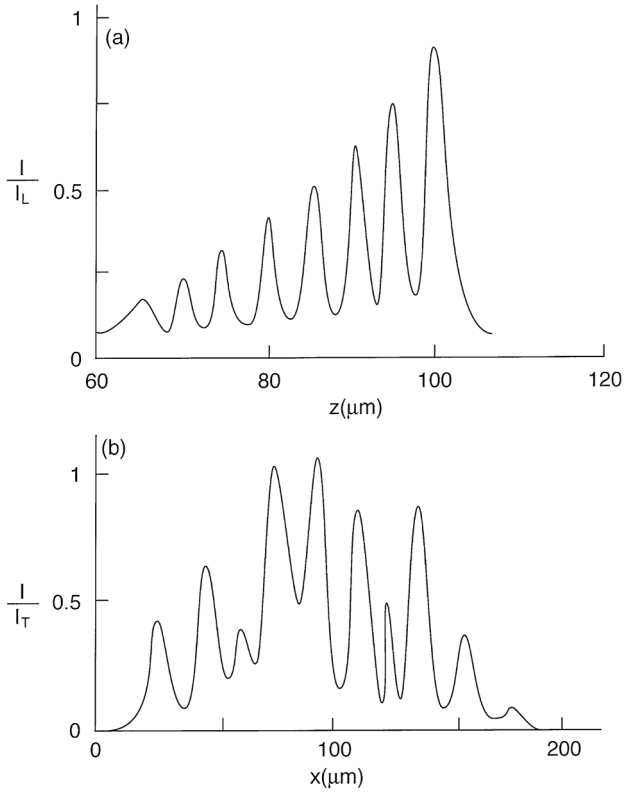

FIG. 2. Plot of laser intensities in (a) the longitudinal z direction and (b) the transverse x direction near the critical surface at $t = 100$ ps. Here $I_L = 9 \times 10^{14}$ W/cm^2 and $I_T = 8 \times 10^{14}$ W/cm^2.

surface and in the conduction zone develops in the ion density. This structure may have important consequences for thermal self-focusing processes. Significant smoothing is observed also for the ion density perturbations from the critical to ablation surface. In addition, the root mean square $\sigma_{\rm rms}$ of the ion density perturbations was computed as a function of the longitudinal direction. The root mean square $\sigma_{\rm rms}$ is given by

$$\sigma_{\rm rms}(z) = \frac{1}{\langle n_i \rangle}\left[\frac{1}{L_X}\int dx (n_i - \langle n_i \rangle)^2\right]^{1/2}, \qquad (6)$$

where L_X is the system size in the transverse x direction and the angle brackets denote spatial average. The ion density perturbations maximize near the critical surface and decrease in magnitude into the overdense region. The ion density perturbations at the ablation surface $\sigma_{\rm rms}(z = z_{\rm abl}) \leq 0.01$. The ion density perturbations at the ablation surface $\sigma_{\rm rms}(z = z_{\rm abl}) \propto \tau_c^n$ with $n \simeq 0.8$–1 for $\tau_c \simeq 2$–8 ps. The laser coherence time needed for significant smoothing is less than approximately 3 ps. The ion density perturbations were also computed using a Spitzer fluid code for two flux limiters, i.e., $f = 0.07, 0.1$. It was found that the FP model predicts more smoothing than a hydrodynamic model for both flux limiters, i.e., $\sigma_{\rm rms}^{\rm FP} < \sigma_{\rm rms}^{\rm SH}$.

In summary, using a fully kinetic 2D Fokker-Planck model, the generation and evolution of ion density perturbations from nonuniform laser deposition in a plasma slab have been studied. It is observed that the smoothing of the electron temperature and ion density perturbations is dependent on the laser coherence time. It is found that significant smoothing of the ion density perturbations

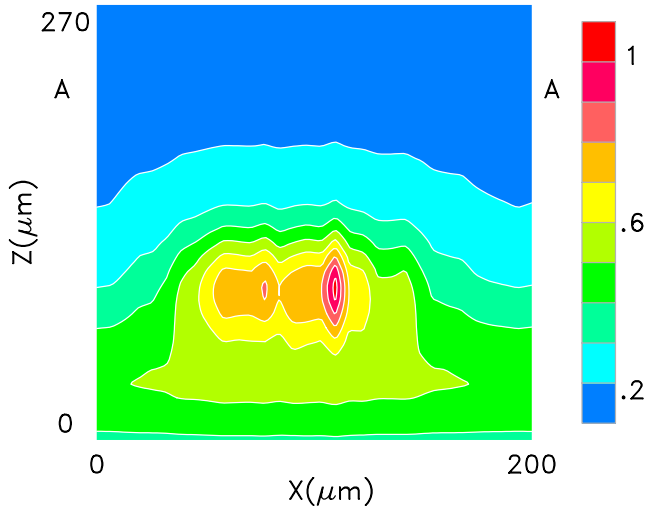

FIG. 3 (color online). Plot of 2D variation of FP electron temperature T_e vs x and z at $t = 420$ ps. Temperature has been normalized by 2.2 keV. The symbol A denotes ablation surface.

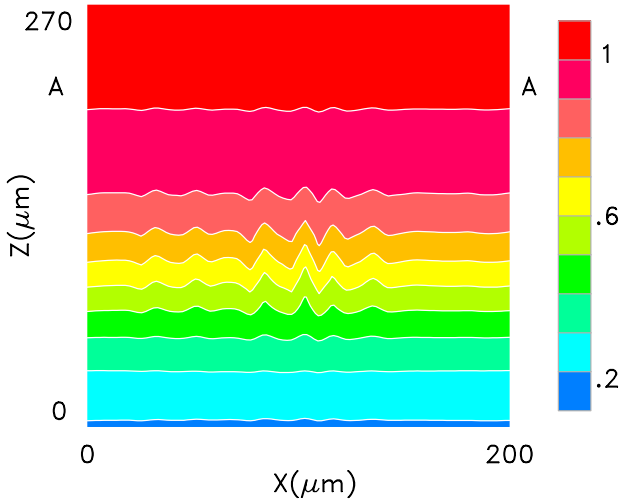

FIG. 4 (color online). Plot of 2D variation of FP ion density at $t = 420$ ps. The density has been normalized by the maximum.

from nonuniform optically smoothed single beam laser deposition can be achieved on hydrodynamic times scales over a range of scale sizes. In addition, it is observed that the Fokker-Planck model predicts more smoothing than the hydrodynamic Spitzer model.

We thank Andy Schmitt, S. Obenschain, D. Colombant, W. Manheimer, and J. Bates for useful discussions. This work was supported by the U.S. Department of Energy.

[1] J. D. Lindl, *Inertial Confinement Fusion* (Springer-Verlag, New York, 1998).
[2] S. E. Bodner, J. Fusion Energy **1**, 221 (1981).
[3] M. H. Emery, J. H. Orens, J. H. Gardner, and J. P. Boris, Phys. Rev. Lett. **48**, 253 (1982).
[4] J. H. Gardner and S. E. Bodner, Phys. Rev. Lett. **47**, 1137 (1981).
[5] R. H. Lehmberg and S. P. Obenschain, Opt. Commun. **46**, 27 (1983).
[6] S. Skupsky, R. W. Short, T. Kessler, R. S. Craxton, S. Letzring, and J. M. Soures, J. Appl. Phys. **66**, 3456 (1989).
[7] Y. Lin, T. J. Kessler, and G. N. Lawrence, Opt. Lett. **21**, 1703 (1996).
[8] W. L. Kruer, Comments Plasma Phys. Controlled Fusion **9**, 63 (1985); G. Schurtz *et al.*, Phys. Rev. Lett. **98**, 095002 (2007).
[9] W. Manheimer, Phys. Fluids **20**, 265 (1977).
[10] M. Straus, G. Hazak, D. Shvarts, and R. Craxton, Phys. Rev. A **30**, 2627 (1984); A. V. Brantov *et al.*, Phys. Plasmas **10**, 4633 (2003); Ph. Nicolai *et al.*, Phys. Plasmas **13**, 032701 (2006).
[11] J. Matte and J. Virmont, Phys. Rev. Lett. **49**, 1936 (1982).
[12] J. Matte, T. W. Johnston, J. Delettrez, and R. L. McCrory, Phys. Rev. Lett. **53**, 1461 (1984).
[13] J. Luciani, P. Mora, and J. Virmont, Phys. Rev. Lett. **51**, 1664 (1983).
[14] J. Albritton, Phys. Rev. Lett. **50**, 2078 (1983).
[15] G. J. Rickard, A. R. Bell, and E. M. Epperlein, Phys. Rev. Lett. **62**, 2687 (1989).
[16] E. Epperlein, G. Rickard, and A. Bell, Phys. Rev. Lett. **61**, 2453 (1988).
[17] A. Sunahara, J. Delettrez, J. Stoeckl, R. Short, and S. Skupsky, Phys. Rev. Lett. **91**, 095003 (2003).
[18] V. K. Senecha, A. V. Brantov, V. Yu. Bychenkov, and V. T. Tikhonchuk, Phys. Rev. E **57**, 978 (1998).
[19] O. V. Batishchev, V. Yu. Bychenkov, F. Detering, W. Rozmus, R. Sydora, C. E. Capjack, and V. N. Novikov, Phys. Plasmas **9**, 2302 (2002).
[20] J.-L. Feugeas, Ph. Nicolaï, X. Ribeyre, G. Schurtz, V. Tikhonchuk, and M. Grech, Phys. Plasmas **15**, 062701 (2008).
[21] I. R. Williams, G. J. Rickard, and A. R. Bell, Laser Part. Beams **9**, 247 (1991).
[22] I. Shkarofsky, T. Johnston, and M. Bachynski, *The Particle Kinetics of Plasmas* (Addison-Wesley, Reading, MA, 1966).
[23] A. Langdon, Phys. Rev. Lett. **44**, 575 (1980).